Intelligent Traffic Flow Predictive Control Based on Multi-Node Bilateral Control Model in Closed Congested Road Scenarios

Xiliang Wang, Huijian Geng*
School of Traffic and Transportation, Shijiazhuang Tiedao University, Shijiazhuang 050043, China
E-mail: wangxiliang263@sina.com, zhangjessie19@sina.com
*Corresponding author

Keywords: congested roads, multi-node bilateral control, intelligent transportation, flow control, conditional generative adversarial network

Received: July 18, 2024

With the increase in urban population and the popularization of transportation, traffic flow control has become a key issue in urban traffic management. This requires researching a new intelligent traffic flow control method to improve the efficiency and sustainability of the transportation system. Based on this, this study proposes an intelligent traffic flow control method based on a multi-node bilateral control model. This method adopts the Kalman filter algorithm to intelligently regulate intersection flow, considering the mutual influence between multiple nodes, and optimizing traffic flow through coordinating the traffic flow on both sides of the road intersection. The results showed that the designed traffic flow control prediction model could improve the accuracy of traffic flow prediction to 84.7% during training and testing. The recognition accuracy of pedestrian targets could be improved to over 80%. In the case of large traffic flow, the designed model could expand the distance between vehicles to 37.5m, greatly improving driving safety. The multi-node bilateral control model can effectively improve the traffic problems of urban roads, reduce people's travel costs, improve people's travel experience, and promote the economic development of urban roads.

Povzetek: Predlagan je nov pristop inteligentnega nadzora prometnega toka z večvozliščnim bilateralnim modelom, ki z uporabo Kalmanovega filtra izboljša napovedi ter poveča varnost in učinkovitost v prometnih zastojih.

1 Introduction

In today's urban transportation system, closed and congested road scenes are common problems, which pose higher requirements for Traffic Flow Control (TFC). The urbanization process and the increase in private cars have made traffic congestion a common problem, and traditional infrastructure cannot meet the rapidly growing demand for transportation. This situation not only wastes time and resources but also raises environmental and safety issues. However, the rapid advancement of information and communication technology has enabled the implementation of intelligent traffic management systems. By applying sensors, cameras, and big data technology, real-time monitoring of traffic conditions can be achieved, and intelligent algorithms can be used for traffic scheduling and optimization [1]. In the current research on Intelligent Traffic Flow Control (ITFC), there are already real-time control, machine learning algorithms, and optimization algorithms based on sensor data [2-4]. However, challenges still exist in terms of stability, data requirements, and interpretability. In addition, as an application of real-time coordination of intersection nodes and intelligent decision-making algorithms, Multi-Node Bilateral Control (MNBC) has made significant progress in traffic network optimization, real-time data application, intelligent decision-making, and adaptive optimization [5]. Based on this, this study proposes an ITFC method based on the MNBC model. This method uses advanced control algorithms to intelligently regulate intersection traffic. It considers the mutual influence between multiple nodes and optimizes traffic flow through bilateral control strategies. This study aims to explore how to optimize traffic flow, improve road capacity, and reduce the adverse effects of traffic congestion on urban socio-economic development.

The innovation of the research includes the following two points. First, the Kalman filter state estimation method has been used to improve the state estimation method during vehicle driving. The second point lies in utilizing Doppler features to improve pedestrian feature extraction and recognition. In conventional traffic flow prediction, vehicle status is mostly transmitted in real-time through sensors, which is costly. The proposed method does not employ vehicle sensors and instead utilizes Kalman filtering to calculate and update the vehicle status. The main contribution of the research is to improve the accuracy of urban traffic flow prediction models in complex environments, propose control methods for peak traffic flow periods, improve the load capacity of urban transportation networks, and strengthen the level of urban

transportation.

The overall structure of the study is divided into four parts. The first part is the literature survey of the research topic and research method of the article. The second part is the study on the construction of the MNBC model. The third part is the experimental verification of the MNBC model. The fourth part is the summary of the research content.

2 Related works

Urbanization and population growth have brought about an increasing demand for transportation, leading to problems such as traffic congestion and decreased intersection efficiency. To address these issues, some scholars have conducted a series of studies. Du et al. proposed a non-local conservation law model aimed at in-depth analysis of inter-vehicle communication in traffic flow. This model was restorative under the equilibrium approximation limit. However, it had a poor effect on the TFC in the complex environment [6]. Zhai and Wu proposed a new grid-based fluid dynamics model for entrance ramps, aiming to provide drivers with traffic flow prediction information. Traffic flow rate and driver prediction time had a significant impact on traffic stability. However, this method had a long response time and poor timeliness in complex environments [7]. Hyochang et al. have proposed a method for integrating automatic license plate recognition in traffic control, aimed at identifying license plates and managing them to build an intelligent traffic management system. This method could recognize license plates in various complex environments, thereby implementing intelligent management of vehicles coming and going. This method proved ineffective in controlling traffic flow and is therefore only suitable for the management of entry and exit points [8]. Finkelberg et al. investigated the potential impact of temporarily reducing communication channel reliability on intersection capacity, aiming to use vehicle information to inform intersection controllers about the location and speed of connected vehicles. This method reduced delays at isolated and connected intersections in all cases. However, the author did not design how to use the vehicle information to achieve TFC [9]. Epitia, N et al. proposed an event-triggered output feedback controller to stabilize traffic flow on two connected roads. This controller was based on a linearized Aw Russell Zhang model and utilized ramp control strategies to regulate traffic flow rates. The results showed that the controller ensured exponential convergence of the closed-loop system, effectively suppressed traffic oscillations, and avoided the Zeno phenomenon, but it could not alleviate urban traffic congestion [10]. To fully understand how autonomous vehicles smooth traffic flow, Heng. Y et al. studied the controllability, stability, and accessibility of hybrid traffic systems from the perspective of control theory. It was proposed that the hybrid traffic system was not completely controllable but stable, and the traffic speed could be increased by controlling autonomous vehicles. The results showed that only 5% of autonomous vehicles could increase the traffic speed by more than 6%, which verified the great potential of autonomous vehicles in smoothing traffic flow. However, autonomous driving technology was not yet mature and could not be applied on a large scale [11].

Liu Q et al. proposed a traffic prediction model that combines graph convolutional networks and long short-term memory networks to address the transportation challenges brought about by urbanization. The results showed that the model exhibited high prediction accuracy and reliability on the Cangzhou traffic dataset, but the method could not control changes in traffic flow [12]. Yu J proposed a long short-term memory network prediction model based on differential evolution and grey wolf optimization algorithm optimization to improve the traffic conditions in scenic spots and reduce travel time costs. The results showed that the model significantly improved the accuracy of passenger flow prediction and provided strong support for the healthy development of the tourism industry. However, the model could only predict changes in traffic flow in scenic spots [13]. Ge, X et al. proposed a dynamic event-triggered scheduling method to balance control performance and resource efficiency in distributed coordinated control. The results showed that this method could dynamically adjust the triggering mechanism based on system information and dynamic variables, and has been applied in the fields of microgrids and automatic vehicles [14]. Pu. S et al. proposed a gradient partial distributed control method to solve the problem of high cost in distributed convex optimization. The results showed that this method could improve the convergence of the convex function objective function under multiple variants and asynchronous random gossip settings [15]. The summary results of the relevant working survey literature are shown in Table 1.

Table 1: Summary results of the survey literature

Author	Method	Insufficient
Du, Q. et al.	Non local conservation law model	Not suitable for complex environments
Zhai, C. et al.	Grid based fluid dynamics model for entrance ramps	Not suitable for complex environments
Hyochang, A. et al.	License Plate Recognition Traffic Control	Unable to control traffic flow

Finkelberg, I. et al.	Vehicle Information Extraction Model for Transportation Network	Unable to control traffic flow
Espitia, N. et al.	Ramp control strategies	Unable to alleviate traffic pressure
Zheng, Y. et al.	Analyzed the potential of autonomous driving	Autonomous driving technology cannot alleviate traffic pressure
Liu, Q. et al.	Graph Convolutional Networks and Long Short-Term Memory Networks	Unable to control traffic flow
Yu, J.	Long Short-Term Memory Network Prediction Model Optimized by Differential Evolution and Grey Wolf Optimization Algorithm	Unable to control traffic flow
Ge, X. et al.	Dynamic event triggered scheduling method	Not suitable for complex environments
Pu, S. et al.	Partial distributed control method for gradient field	Not suitable for complex environments

In summary, in recent years, TFC has made significant progress by combining various technical methods such as deep learning, dynamics, and automatic recognition. The current TFC method has the problems of slow control response and more control effect. However, MNBC takes into account factors both inside and outside the intersection, surpassing the traditional focus on controlling traffic lights within the intersection. This method broadens the perspective while considering the flow and status of roads around intersections, which helps to improve the limitations of traditional traffic control. Therefore, the research on intelligent traffic flow based on the MNBC model has practical significance for improving TFC.

3 Traffic flow control method for MNBC model

This study proposes a Predictable Bilateral Control Model (PBCM) by deeply analyzing the error and Zdelay problems that vehicle systems may encounter in actual operation. This model utilizes the Kalman idea for optimal estimation while obtaining the system's prediction quantity through the prediction process. Next, the micro-Doppler waveforms generated by pedestrians during walking are introduced, as well as how to achieve denoising by setting energy thresholds. To solve the problem of pedestrian recognition, an algorithm based on deep Convolutional Neural Networks (CNN) is proposed, and data augmentation methods are planned to address the insufficient dataset.

3.1 Building a bilateral control model with kalman filter fusion

The core idea of the bilateral control model is to optimize traffic flow by coordinating signal control on both sides of intersections or other traffic nodes [16, 17]. This model mainly focuses on the collaborative effect between adjacent nodes to maximize road traffic efficiency and alleviate traffic congestion. Fig. 1 shows the physical abstraction model of the bilateral control system.

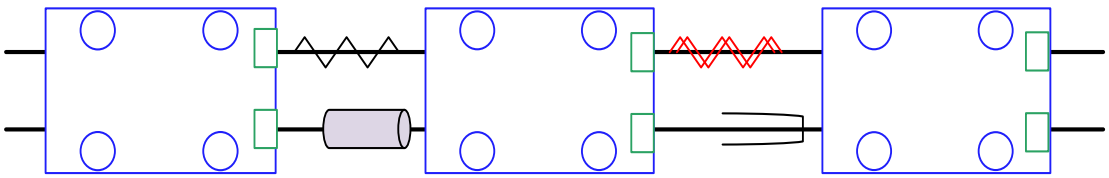

Figure 1: Physical abstract model of bilateral control system

In Figure 1, the study assumes that the front and rear spacing is consistent when the distance between the vehicles does not affect the vehicle acceleration. However, the acceleration is inversely proportional to the relative speed of the current vehicle and the front and rear vehicles. The abstraction of the system can be seen as a connection between a vehicle of a particular length and a damper. The deformation of the spring is proportional to the force applied, while the force applied to the damper is proportional to the velocity. In a given one-way vehicle road model, vehicles are assumed to travel on the road, while ignoring any environmental factors in the ideal scenario [18]. The mass of each vehicle is m, and the Hooke's coefficient of the spring is k_d. The total energy E of the system can be expressed by considering the contributions of kinetic energy and elastic potential energy, as shown in Equation (1).

$$E = \frac{1}{2}\sum_{i=1}^{N-1} m\dot{x}_i^2 + \frac{1}{2}k_d \sum_{i=1}^{N-1}(x_{i+1} - x_i)^2 \quad (1)$$

In Equation (1), $\dot{x}$ represents the derivative of displacement. Assuming that the mass of all vehicles in the vehicle system is equal and constant, the mass can be set to 1. Derivative operations are performed on the above energy expression, as shown in Equation (2).

$$\frac{dE}{dt} = \sum_{i=1}^{N-1} \dot{x}_i \ddot{x}_i + k_d \sum_{i=0}^{N-1}(x_{i+1} - x_i)(\dot{x}_{i+1} - \dot{x}_i) \quad (2)$$

In Equation (2), $\ddot{x}$ represents the second derivative of displacement. Equation (1) is substituted into Equation (2), and Equation (2) is simplified to the right of the equal sign, resulting in Equation (3).

$$\sum_{i=1}^{N-1} \dot{x}_i \ddot{x}_i + k_d \sum_{i=0}^{N-1}(x_{i+1} - x_i)(\dot{x}_{i+1} - \dot{x}_i) = -k_d \sum_{i=0}^{N-1} \dot{x}_i (x_{i+1} - 2x_i + x_{i-1}) \quad (3)$$

The velocity and acceleration are written as derivatives, and the acceleration is substituted into Equation (2) to obtain Equation (4).

$$\frac{dE}{dt} = -k_d \sum_{i=0}^{N-1}(x_{i+1} - x_i)^2 \quad (4)$$

For system stability, it is required that all vehicles have the same speed, i.e.

$$\frac{dE}{dt} = 0.$$

Due to zero acceleration, the distance between vehicles remains constant, and the system reaches a stable state. Kalman filter algorithm is an effective recursive filter, mainly used for state estimation in linear dynamic systems. The algorithm can estimate the state variables of dynamic systems based on a series of noise-containing observation data to provide the optimal estimation of states such as position, speed, etc. Kalman filtering is particularly suitable for systems handling continuous, linear, and containing Gaussian noise. The Kalman filtering algorithm is adopted to estimate the system state and handle dynamic systems with noise and uncertainty [19]. Through this filtering, an estimate of the true state of the system can be obtained from unreliable measurement data. This study defines matrices F_k, H_k, Q_k, and R_k for each moment k. For systems with control parameters, it is also necessary to define matrix B_k. The basic assumption of the Kalman model is that the system state at time k evolves from the previous state and follows a certain transition law, as shown in Equation (5).

$$X_k = F_k X_{k-1} + B_k + w_k \quad (5)$$

In Equation (5), F_k represents the transition matrix of the system. B_k indicates that the system is affected by control information. w_k is the process noise, and its distribution conforms to $w_k(0, Q_k)$. At time k, the measured value of the true state satisfies Z_k.

$$Z_k = H_K X_K + V_K \quad (6)$$

In Equation (6), Z_k represents the observation model used to map the actual state space of the system to the observation space, and V_K satisfies $V_K(0, R_k)$. The vehicle system designed in this study will be based on highways, covering vehicles numbered from 1 to N, operating on one-way roads. All vehicles run in the same direction, initially evenly distributed within a certain length range on the road, with an initial vehicle spacing of d_0 and an initial vehicle speed set as acceleration. The dynamic characteristics of the system can be described by the position, velocity, and acceleration of the vehicle. Figure 2 shows a PBCM. In Figure 2, Process Variables (PV) and Set Values (SV) are fundamental variables and parameters in vehicle control. PBCM is used for TFC, with the ability to predict future traffic conditions and support bidirectional information transmission and control. This model achieves predictions through historical data, model predictions, or real-time sensor data while allowing the system to obtain information from different directions to make corresponding adjustments to optimize traffic flow and improve system performance. The training and testing process of the bilateral control model mainly includes the following steps: Step 1 is to collect samples containing images and micro-Doppler data, and adjust and denoise them in the preprocessing stage. Then, a CNN is used to extract visual features from the image, as well as features such as velocity and direction from the micro-Doppler data. These features are fused into a unified feature vector and input into the CNN model for pedestrian detection and recognition. In addition, a Conditional Generative Adversarial Network (CGAN) is introduced in the study to generate micro-Doppler images of pedestrians to expand the training dataset and improve the model's generalization ability. During the

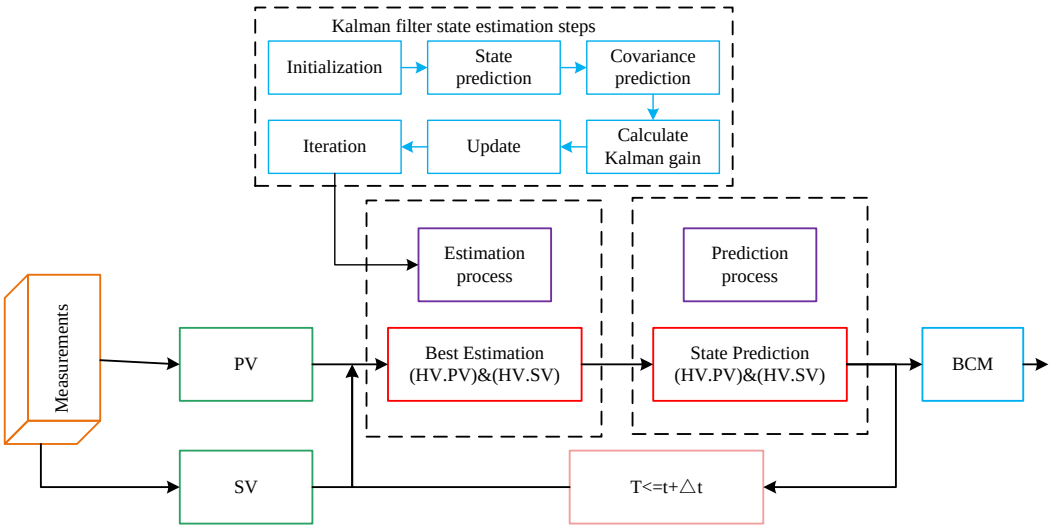

Figure 2: Predictive bilateral control model

training process, the model is optimized through multiple iterations, and the validation set is used to adjust parameters to improve performance. The final step is to evaluate the model on an independent test set to ensure good performance on unseen data. Implementation methods may include intelligent traffic signals, real-time traffic monitoring, sensor-based predictive analysis, and other technologies. The delay caused by the system is usually between 50ms and 120ms, denoted as t_{sys}. Considering the delay caused by communication and the system, the total delay of the vehicle system is defined as t_{total}, and the specific expression is Equation (7).

$$t_{total} = t_{comm} + t_{sys} \tag{7}$$

In equation (7), t_{comm} represents system communication delay. In the bilateral control system, this study only considers the front and rear vehicles of the current vehicle. After obtaining the vehicle status with the bilateral control system, the vehicle control decision can be made according to the vehicle status information to realize the TFC. Introducing the MNBC model can further enhance the credibility of control decisions. Unlike traditional bilateral control models that only consider two directly adjacent vehicles (i.e. direct front and rear vehicles), in the MNBC model, the current vehicle utilizes the state information of k vehicles before and after each. By integrating the information of these $2k$ vehicles, control decisions can be made more effectively. Specifically, for the information of these $2k$ vehicles, the current acceleration a of the vehicle can be calculated using Equation (8).

$$a_n = k_d\left(\sum_{m=-k}^{k} g_m x_{n-m}\right) + k_v\left(\sum_{m=-k}^{k} h_m v_{m=n-m}\right) \tag{8}$$

In Equation (8), symbol a represents the acceleration of the current vehicle. x represents the position information of k adjacent vehicles in front and behind. v represents the speed information of k adjacent vehicles in front and behind. This study assigns weights to the information of each vehicle based on the distance between them, and satisfies the expression in Equation (9).

$$\sum_{m=-k}^{k} g_m = 0 \; and \; \sum_{m=-k}^{k} g_m m = 0 \tag{9}$$

In Equation (9), symbols g and h respectively represent weights related to the distance of the current vehicle.

3.2 Pedestrian recognition method based on micro-doppler features

The pedestrian is a very important link in road traffic. Road traffic flow pedestrian proficiency is a direct concern. The more pedestrians in road traffic, the more crowded the road traffic will be, and the more difficult it is to control. Therefore, when controlling the road traffic flow, the pedestrian situation in the road traffic must be the focus. The Micro-Doppler Characteristics (MDC) of pedestrians refer to the small Doppler frequency shifts caused by pedestrian movement, which can be detected by radar or other sensors. The micro-Doppler effect is the frequency change caused by the movement of a moving target relative to the observer. For pedestrians, MDC can provide information about their motion status, such as speed, direction, and acceleration [20]. When the radar and target are relatively stationary, the signal wavelength is equal. However, in practice, due to relative motion, the

wavelength of the target becomes longer (red-shift) when it moves away from the radar, and shorter (blue-shift) when it approaches, causing the Doppler effect. The calculation of Doppler frequency shift is given by Equation (10).

$$f = \frac{2v}{c} f_1 \tag{10}$$

In Equation (10), f_1 represents the carrier frequency of the radar. v represents the relative velocity between the radar and the target. c represents the propagation speed of electromagnetic waves. The pedestrian recognition method in this study utilizes MDC-based data. These data come from a multi-channel Frequency Modulated Continuous Wave (FMCW) radar with a carrier frequency of 77GHz and a signal bandwidth of 100MHz [21]. In FMCW radar, by transmitting one frequency modulation sequence signal at a time, the time-domain expression of the transmitted signal is calculated by Equation (11).

$$s(t,1) = \exp(j2\pi(f_B t - f_D . l T_{chirp} + \Phi)) \tag{11}$$

In Equation (11), l represents the serial number of the frequency modulation signal, and $l \in [1, L]$. f_D represents Doppler frequency, and Φ represents the randomness of phase. The duration of the frequency modulation radar signal sequence is represented by T_{chirp}. After the signal is irradiated on a pedestrian target, the Doppler frequency f_D of the reflected echo contains multiple components. Each component corresponds to a different body part of the target. The time domain of the echo signal is given by Equation (12).

$$s(t,1) = \sum_{k=1}^{K} \exp((j2\pi(f_B t - f_{D,k} . l T_{chirp} + \Phi_k)) \tag{12}$$

In Equation (12), l represents the serial number of the frequency modulation signal and $l \in [1, L]$. K is the number of target radar reflection points. $f_{D,k}$ represents the Doppler frequency at the reference reflection point K. Sigmoid is an activation function widely used in the early stages of deep neural networks, as shown in Equation (13).

$$f(z) = \frac{1}{1 + e^{-z}} \tag{13}$$

In Equation (13), e represents a natural function, and $f(z)$ represents the output relative to input z. The expression of the Relu function is given by Equation (14).

$$\mathrm{Re}lu(x) = \max(0, x) \tag{14}$$

In Equation (14), $\max(0, x)$ represents the maximum value taken between the relative inputs 0 and x. The Leaky Relu function is given by Equation (15).

$$f(x) = \max(ax, x) \tag{15}$$

In Equation (15), $\max(ax, x)$ represents the maximum value taken between ax, x. The CNN pedestrian recognition structure used in this study is shown in Figure 3.

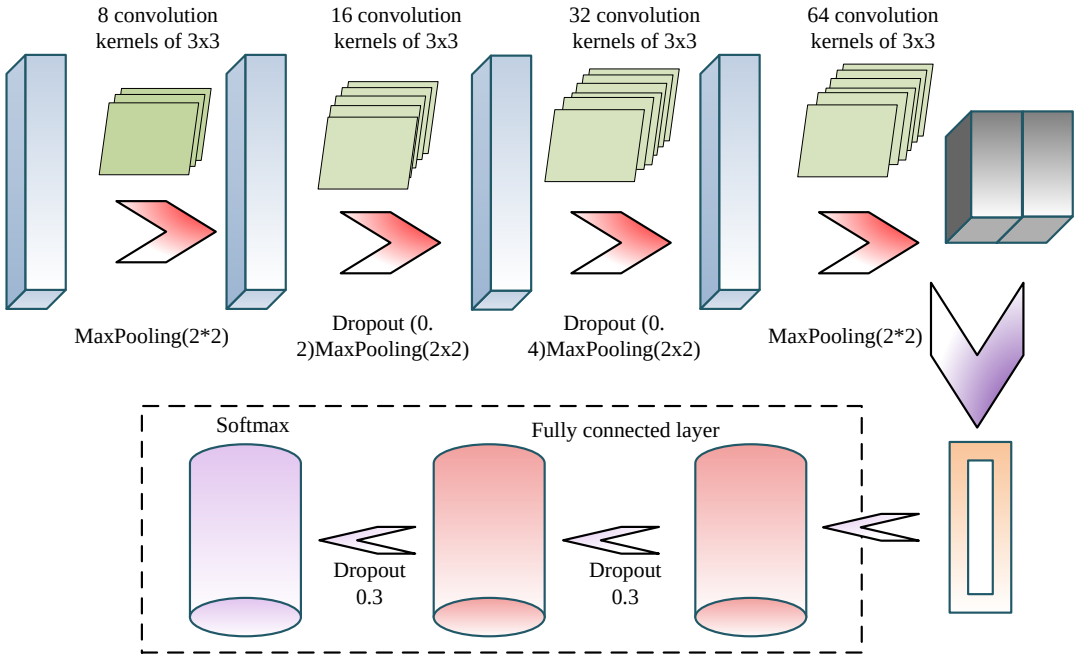

Figure 3: Specific parameters of pedestrian recognition network structure

Figure 3 shows a pedestrian recognition method that integrates CNN and MDC to improve accuracy by combining image and radar data [22]. Doppler data are collected using high-frequency FMCW radar, which reflects the MDC of pedestrian movement. The collected raw data will undergo preprocessing, including adjustment and denoising, to improve data quality. Subsequently, these data are used to train a CNN, which performs pedestrian detection and recognition by extracting features from images and Doppler data. To enhance the generalization ability of the model and expand the training dataset, researchers also use CGAN to generate simulated pedestrian Doppler images. By combining the data generated by CGAN with real data and training the CNN model, the accuracy of pedestrian recognition is further improved. Finally, the trained model is deployed in an actual traffic management system and continuously monitored and optimized to ensure its effectiveness. Firstly, this study collects samples containing images and micro-Doppler data and adjusts and denoises them during the preprocessing stage. Next, CNN extracts visual features from the image, while also extracting features such as velocity and direction from micro-Doppler data. These features are fused into a unified feature vector and input into a CNN model for pedestrian detection and recognition. In terms of Generative Adversarial Network (GAN), standard GANs can generate realistic images but are usually unlabeled, and the training process may be uncontrollable. To address this issue, a CGAN is introduced, which can generate labeled data. This study further introduces the Assisted Classification GAN (ACGAN), which enables it to generate multi-class data and expands the application scenarios of GAN. The research task is to generate micro-Doppler images of different pedestrians walking, and the overall architecture is shown in Figure 4.

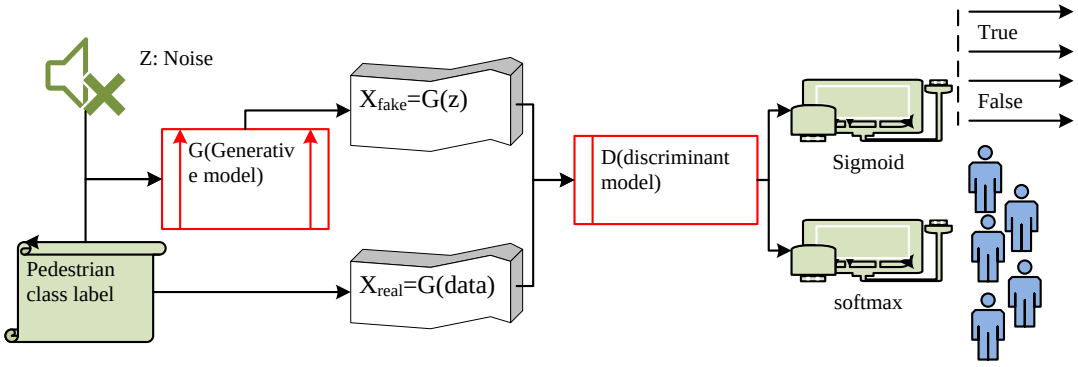

Figure 4: Schematic of the ACGAN used in this article

In Figure 4, the main focus is on the data generator and data discriminator, and it is necessary to specifically determine the form of the discriminant model and the generated model. This study mainly uses CNN. Due to the involvement of both truth and falsehood detection and classification in the task, this study connectsa Softmax classifier and a classifier specifically designed for binary classification after the convolutional layer. For generative models, the research objective is to generate images based on random noise. Usually, this simulates the process of sample generation through fully connected layers and deconvolution layers. In each layer, this study addsbatch normalization processing to improve the stability of the model. The parameters and hierarchical structure of the discrimination model are shown in Figure 5. In Figure 5, the parameters of the discriminative model typically include the weights and bias terms of the convolutional layer, as well as the weights and bias terms of the fully connected layer. These parameters are adjusted during the training process through backpropagation and optimization algorithms to enable the discriminative model to accurately distinguish the authenticity of the generated images or data. This study uses a CNN-based network structure to predict the micro-Doppler of pedestrians at the next moment through Doppler data. These data are about the walking behavior of pedestrians over some time, so there is a certain temporal correlation. The training process of the CNN-based prediction model is shown in Figure 6.

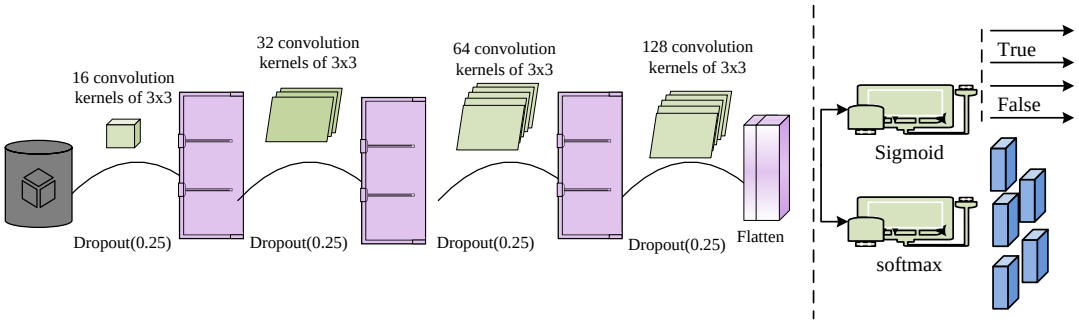

Figure 5: Parameter diagram of discriminant model

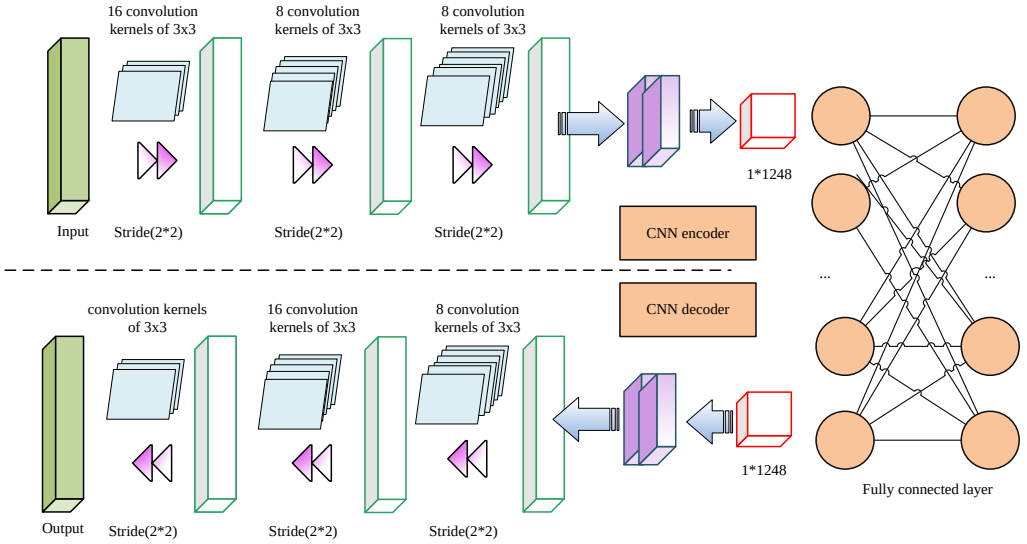

Figure 6: Training process of predictive model based on CNN

In Figure 6, the training of the CNN-based prediction model includes steps such as data preparation, preprocessing, model construction, training, validation, testing, deployment, and monitoring. Firstly, this study collects Doppler data and target labels and normalizes the data. Then, appropriate activation and loss functionsare selected to construct the CNN model. The modelis optimized through multiple trainings, and the validation set is used to adjust parameters to improve performance. Finally, the model is evaluated on an independent test set to ensure that it performs well on unseen data. After completing the training, the model is deployed to practical applications and regularly monitored and updated to ensure effectiveness.

4 TFC performance verification of MNBC model

This experiment is divided into two parts: traffic flow simulation and pedestrian recognition. A simulation platform is established using Java, which has a visual vehicle system operation system, supports real-time data collection and parameter settings, and increases experimental authenticity. For pedestrian recognition, Tensor Flow is chosen as the development platform, utilizing its efficiency and dynamic calculation graph characteristics. The experiment is run on a machine with AMD 2600x CPU, rx580 GPU, and 32GB of memory.

4.1 Experimental implementation of predictability bilateral control model

In the simulation system, all vehicles run on a circular road with a length of 1500 meters. The length of each vehicle is fixed, and they travel at a specific fixed speed when the system is activated. To make it easier to distinguish adjacent vehicles, this study uses three different colors to identify them. Assuming that each vehicle is equipped with an FMCW millimeter wave radar module and V2V communication module, this means that each vehicle can obtain relevant parameters about its operating status through sensors. Table 2 shows the initial parameters of the system.

Table 2: Relevant parameters of the simulation system

Name	Value	Name	Value
System simulation duration	500s	Expected velocity feedback gain	Kc = 0.01
Maximum/small acceleration	a =±3 m/s^2	Vehicle initialization speed v_0	30 m/s
Front and rear relative velocity feedback gain	k_v = 0.2	Initial vehicle spacing d_0	37.5 m
Duration per break	t = 2 s	Road width l_2	5 m
Vehicle length l_3	L = 5 m	Number of vehicles N	40
Total road length l_1	1500 m	Distance feedback gain	ka = 0.1

In Table 2, the total length of the road is set to 1500 m, the experimental simulation time is 500 s, the relative speed feedback gains before and after is 0.2, and the expected speed feedback gain is 0.01. On a fixed-length one-way road, uniform spacing between vehicles indicates a more balanced system and lower collision probability, while closer speeds help improve system efficiency. Therefore, this study focuses on the stability of vehicle systems, mainly considering vehicle spacing and speed. In the simulation system, the speed of each vehicle at each momentis obtained. For a system containing N vehicles, a closer speed indicates a lower probability of collision. TAPAS Cologne Dataset sources from the Cologne transportation project. It provides traffic flow simulation data in a virtual urban environment, including vehicle trajectory and signal status, suitable for the development and testing of traffic simulation and management systems. The dataset is the simulated experiment of MNBC. The study first compares the control situation of different control systems. Among them, cases 3, 7, and 15 are three different control systems, and the differences are obvious. Therefore, the study collects the speed data of cases 3, cases 7, and cases 15, and extracts the data from different time points, as shown in Figure 7. Figure 7(a) shows the speed graph of the vehicle controlled by the following model in three scenarios, showing a fluctuating trend at the 9th second. At the 10th second, Case 15 and Case 7 change the control model to a bilateral control model and a PBCM. The car with vehicle ID 5 applies brakes in 10 seconds, and the results show that the following model causes traffic congestion, while the bilateral control model and PBCM perform more stably. Under system control, PBCM exhibits smaller speed differences and greater stability. Figure 8 shows the variation of the minimum workshop distance over time in the vehicle system.

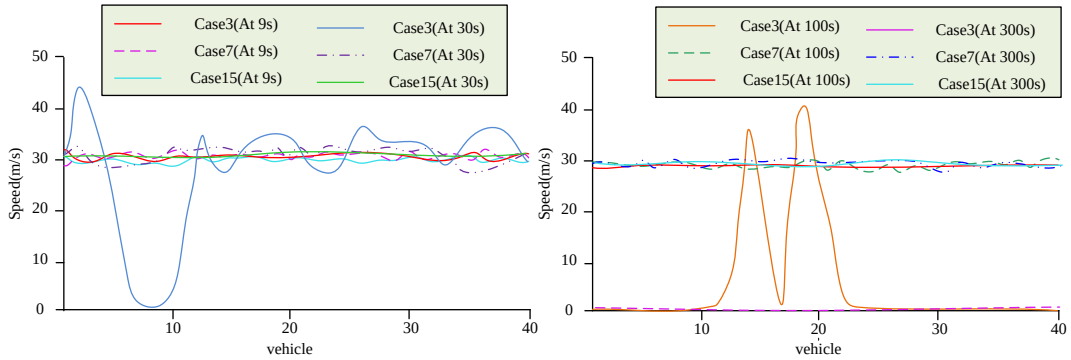

(a) Speed diagram of the system vehicle at 9s and 30s (b) Speed diagram of the system vehicle at 100s and 300s

Figure 7: Vehicle speed during system operation under the control of different models

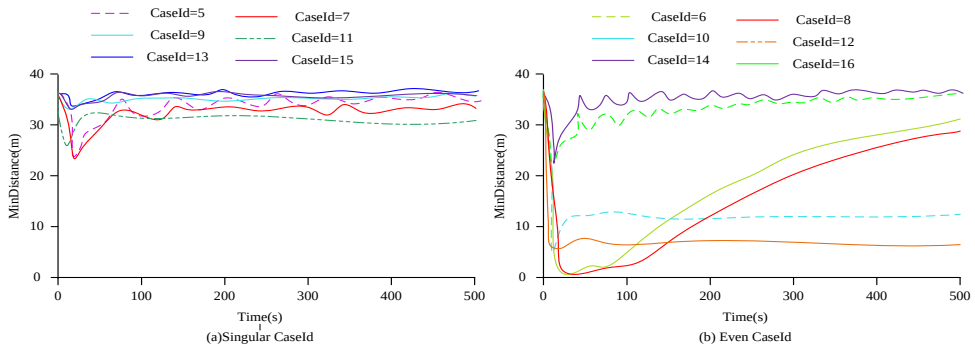

(a)Singular CaseId (b) Even CaseId

Figure 8: Variation of minimum workshop distance with time in vehicle system

In Figure 8, PBCM performs best in various scenarios, with a minimum vehicle spacing of nearly 37.5 m. Taking Figure 8(b) as an example, in the model switching scenario after 2 seconds of braking, bilateral control and MNBC model cause a sharp decrease in the distance between the smallest cars, while PBCM only decreasesfrom 35 m to 33 m. This indicates that in emergency braking situations, the predictive model can better alleviate system disturbances. In Figure 8(a) and 8(b), taking 3% and 5% errors as examples, PBCM maintains a relatively large minimum distance under different error conditions. In contrast, traditional and multi-node models experience a sharp decrease in vehicle spacing after braking. In the case of greater delay (0.2 s), the minimum workshop distance of the predictable model slightly decreases, but it can still quickly recover to a stable state. Meanwhile, traditional and multi-node models require a longer time, and multi-node models are almost unable to operate normally.

4.2 MDC pedestrian recognition experiment

This study explores three methods for measuring the distance between vehicles: minimum distance, maximum distance, and error bars for vehicle spacing. Figure 9 shows the calculation results of the error bar for the minimum distance between vehicles during system operation.

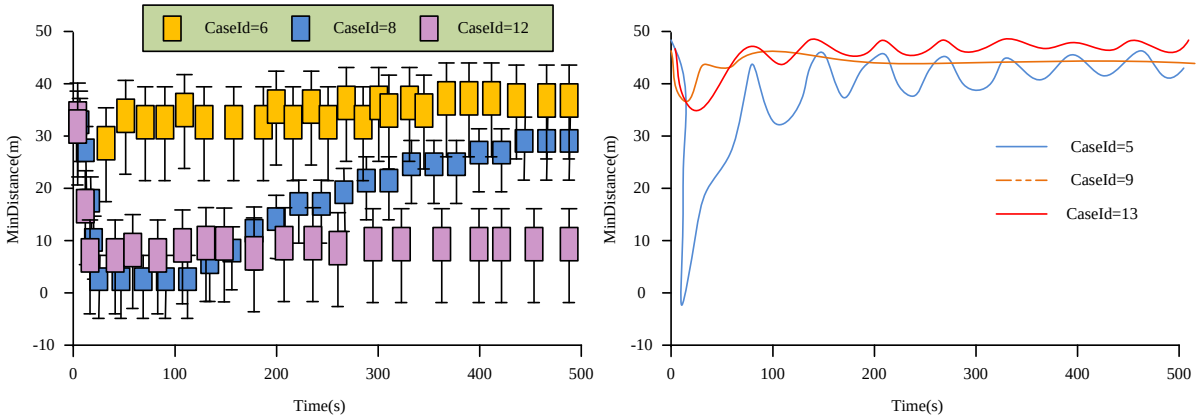

(a) Group A Case (b) Group B Case

Figure 9: Error bar of car spacing in vehicle system

In Figure 9(a) and 9(b), the vehicle system under PBCM control exhibits a smaller error range under both large and small delays and errors. This indicates that under PBCM, the vehicle system is more stable compared to systems under other model controls. Similarly, by collecting data on the maximum vehicle spacing during the operation of the vehicle system and calculating the error range, Figure 10 shows the error range of the maximum vehicle spacing. In Figure 10, compared to the larger maximum vehicle spacing of traditional bilateral control systems and MNBC systems, PBCM can achieve the smallest maximum vehicle spacing (about 39 m) in the vehicle system. This study improves the network structure, including adding a fully connected layer and introducing dropout to prevent overfitting. Figure 11(a) shows the final training result. Extra data are generated through ACGAN and integrated into the training set, with the associated losses presented in Figure 11(b). The data are generated using a CNN model, added to the training set, and then retrained using the CNN model to study the model. Figure 11(c) shows the accuracy during the training process.

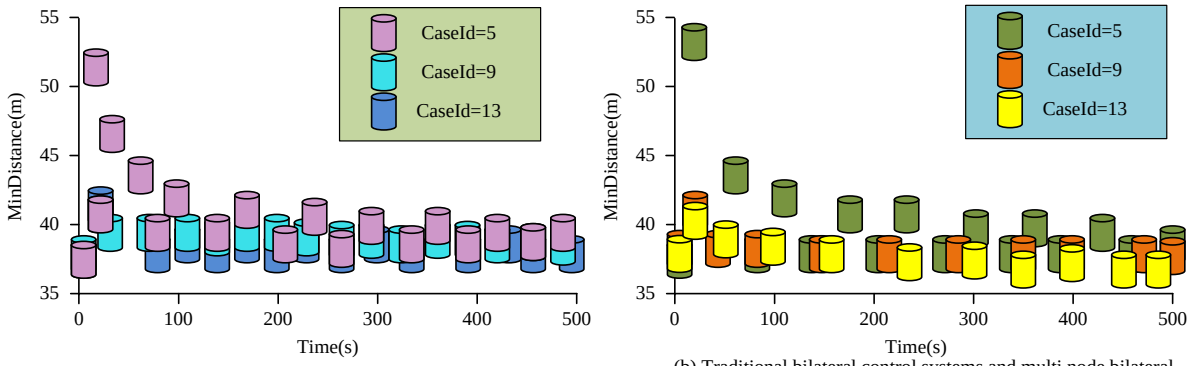

(a) Bilateral control model

(b) Traditional bilateral control systems and multi node bilateral control systems

Figure 10: Maximum spacing and error bar in vehicle system

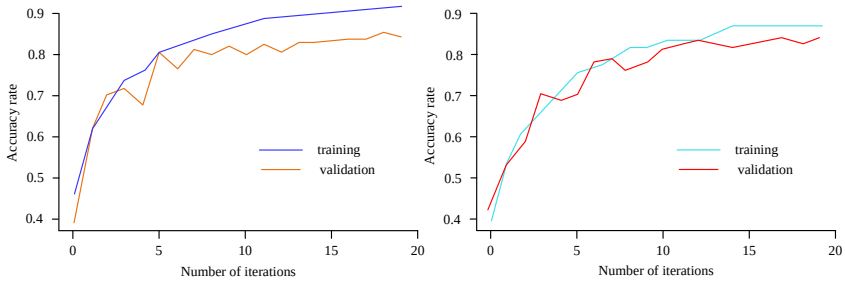

(a) Pedestrian recognition based on CNN - Accuracy of training set and verification set during training

(b) Generative adversarial network - Accuracy of training set and verification set during training

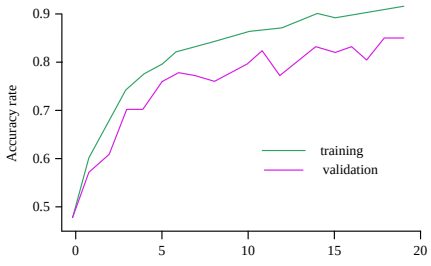

(c) CNN predictive model data augmentation - the accuracy of the training set and validation set during training

Figure 11: Accuracy of training set and verification set during training

In Figure 11(a), a CNN-based prediction model is used for data generation, and the generated data areadded to the training set to retrain the research model using the CNN model. After training, the accuracy ofthe test set is 84.7%. In the research model shown in Figure 11(b), the pedestrian recognition accuracy is approximately 80%. Although improving the network model can improve accuracy, an 80% recognition rate is unacceptable in practical applications. In Figure 11(c), by using ACGAN for data generation and adding the generated data to the training set, the accuracy of the test set is improved from 80% to about 87%, effectively improving the accuracy of pedestrian recognition. In addition, by using a CNN-based neural network for data generation and adding the generated data to the training set, the accuracy of the test set is improved from 80% to about 85%, effectively improving the accuracy of pedestrian recognition. To verify the control effect of this model on traffic flow, the study is compared with the traditional TFC method, and the results are shown in Figure 12. In Figure 12, on a fixed road section, when traditional TFC methods are used for TFC, the number of vehicles passing through per hour is always at a low level, up to 30 vehicles per hour. However, when using the control model proposed in the study, the number of vehicles passing through per hour on this road section is at a high-level during traffic congestion, up to 31 vehicles per hour. The TFC model proposed in the study can effectively improve the congestion situation of urban road traffic during peak hours. The study compares the confusion matrix of pedestrian recognition between CNN and GCAN models in the intersection scene, and the results are shown in Figure 13.

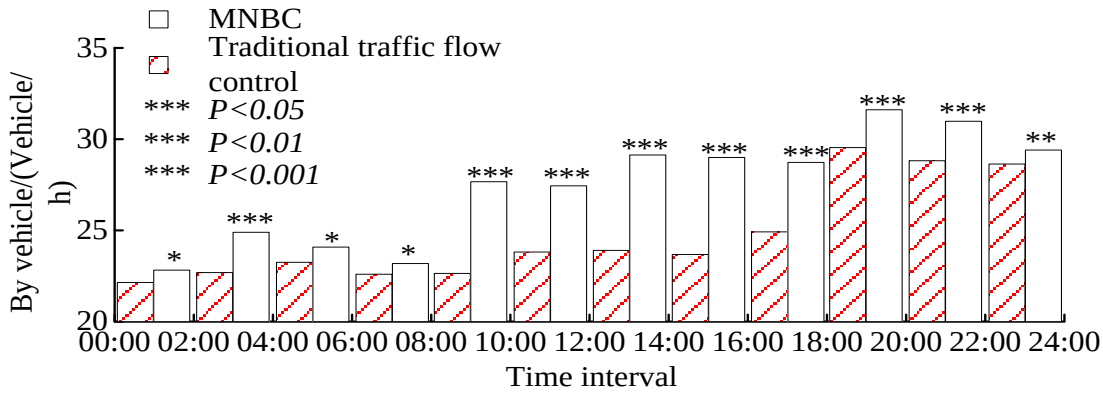

Figure 12: Traffic flow control effect

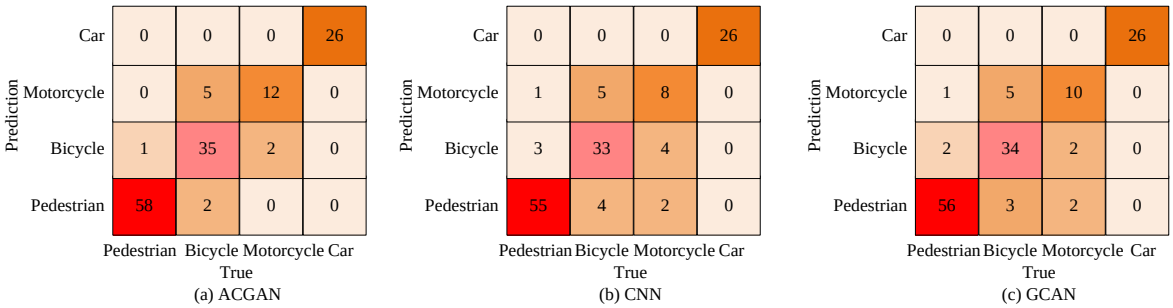

Figure 13: Pedestrian recognition confusion matrix

In Figure 13, the research model only has one case of recognition error in pedestrian recognition results during the recognition process. This model is prone to misidentification when identifying people traveling by bicycle or motorcycle. The frequency of misidentification in CNN and GCAN models during the recognition process is significantly higher than that of the proposed model. A comparative analysis of the response times of different TFC models is performed, and the results are shown in Table 3.

Table 3: Response times of the different traffic flow control models (s)

Time	MNBC	Traditional traffic flow control
7:00~9:00	55	246
11:00~13:00	32	198
17:00~19:00	62	326

As shown in Table 3, the response time of the TFC model is significantly lower than that of traditional TFC schemes during the three peak periods of urban traffic. The response time of the TFC scheme is the highest at 62 seconds, while the response time of the traditional TFC scheme is the shortest at 198 seconds. When deploying the model in larger urban networks, modular design is required for easy management and upgrading. Layered control strategies are implemented to meet different levels of traffic management needs. Data integration and communication infrastructure are strengthened to ensure real-time and accurate information flow. Algorithms are optimized to improve the ability to handle large-scale data. The reliability of the model is verified through simulation and testing. At the same time, the resilience and fault tolerance of the system should be ensured, and user participation and feedback should be encouraged.

5 Discussion

The MNBC model proposed in the study demonstrates superior performance compared to TFC methods discussed in other literature. Especially when dealing with complex traffic scenarios, the MNBC model demonstrates better processing capabilities compared to the vehicle following model, non-local conservation law model, and grid-based fluid dynamics model proposed in references [7] and [8]. The MNBC model integrates Kalman filtering for state estimation and prediction, which can more effectively manage delays compared to traditional models. In emergency braking events, the MNBC model can more proactively predict and adjust delays, reducing the impact on traffic flow. Even under different delay conditions, the MNBC model can better maintain the minimum distance between vehicles. The MNBC model optimizes traffic flow by considering the mutual influence between multiple nodes, a feature that is absent in traditional models. Traditional models usually only focus on isolated intersections or individual nodes, while the MNBC model considers a wider range of transportation networks, thereby achieving more effective traffic flow optimization. This comprehensive approach has resulted in the establishment of a more stable transportation system, as evidenced by the simulation results, which indicate minimal fluctuations in vehicle speed.

The improvement of the performance of the MNBC model relies on more advanced state estimation, more comprehensive consideration of transportation networks, and real-time data for relevant calculations. The application of the Kalman filter in the MNBC model provides significant advantages for state estimation, which can accurately estimate the state of the transportation system even in the presence of noise and uncertainty. A more comprehensive consideration of the transportation network avoids isolating a certain part of the transportation network. The MNBC model can more effectively optimize traffic flow, thereby improving overall performance. Real-time data applications enable the MNBC model to dynamically adjust according to actual conditions, enabling it to quickly respond to changes in traffic conditions and enhance its adaptability and responsiveness.

Although the MNBC model optimizes the level of TFC, its performance in larger and more complex urban transportation networks needs further evaluation. With the increase in network size, computational complexity, and data requirements may become challenges. The effectiveness of the model largely depends on the accuracy and reliability of traffic sensors. Any inaccuracy in sensor data may affect the performance of the model. Further research is needed on how the MNBC model can be integrated with other intelligent traffic management systems to achieve a comprehensive solution. Future research will develop more efficient algorithms for state estimation and prediction to handle larger networks and reduce computational load. In the future, sensor fusion technology will be improved to enhance the robustness of the model to sensor noise and improve overall accuracy. In addition, comprehensive research will explore how to integrate the MNBC model with other traffic management systems to form a more comprehensive traffic control framework.

6 Conclusion

In modern urban traffic management, TFC in closed congested road scenarios has always been a highly anticipated challenge. The advancement of urbanization has made road congestion increasingly prominent. Traditional car following models are prone to traffic congestion when faced with emergency braking and other situations, requiring the search for more intelligent and robust TFC methods. Therefore, this study adopted the MNBC model and combined it with the non-rigid body micro-Doppler effect to conduct a theoretical analysis of pedestrian MDC. In addition, a pedestrian recognition schemewas constructed using a small FMCW radar. To improve accuracy, ACGAN and CNN-based models were used to enhance the data. The experiment showed that by using ACGAN to generate data and adding it to the training set, the accuracy of thepedestrian recognition test set was improved from 80% to 87%. Meanwhile, by using a CNN-based network to generate data and adding it to the training set, the accuracy of the test set was improved from 80% to 85%. After adopting the proposed TFC model, bilateral control and the MNBC model significantly reduced the distance between the minimum vehicles, while PBCM only reduced it from 35 m to 33 m,

effectively improving the traffic flow under crowded conditions. Both methods effectively improved the accuracy of pedestrian recognition. The MNBC model can effectively improve the congestion of urban road traffic and promote the development of urban road traffic. However, the research model regulates the traffic flow, which will compress the traffic flow and put a higher pressure on the urban traffic load. Future studies will optimize the TFC method to improve the congestion state of urban road traffic without squeezing the traffic flow.

Author Contributions

With the increase of urban population and the popularization of transportation, traffic flow control has become a key issue in urban traffic management. This requires the research of a new intelligent traffic flow control method to improve the efficiency and sustainability of the transportation system. X. W. article proposes an intelligent traffic flow control method based on a multi node bilateral control model. This method adopts the Kalman filtering algorithm to intelligently adjust the intersection flow, considering the mutual influence between multiple nodes, and optimizing the traffic flow by coordinating the traffic flow on both sides of the road intersection. H. G. For this study, the MNBC model was used, combined with the non rigid body micro-Doppler effect, to conduct a theoretical analysis of pedestrian MDC, and a pedestrian recognition scheme was constructed using a small FMCW radar. To improve accuracy, models based on ACGAN and CNN were used to enhance the data.

H. G. and X. W. others made significant contributions to the writing of the manuscript.

Availability of data and materials

All data generated or analyzed during this study are included in this published article.

Acknowledgement

School of Traffic and Transportation, Shijiazhuang Tiedao University

References

[1] F. Storani, R. Di Pace, and B. De Schutter, “A traffic responsive control framework for signalized junctions based on hybrid traffic flow representation,” Journal of Intelligent Transportation Systems, vol. 27, no. 5, pp. 606-625, 2023. https://doi.org/10.1080/15472450.2022.2074790

[2] F. Tajdari, and C. Roncoli, “Online set-point estimation for feedback-based traffic control applications,” IEEE Transactions on Intelligent Transportation Systems, vol. 24, no. 10, pp. 10830-10842, 2023. https://doi.org/10.1109/TITS.2023.3274233

[3] Z. Ning, J. Huang, and X. Wang, “Vehicular fog computing: enabling real-time traffic management for smart cities,” IEEE Wireless Communications, vol. 26, no. 1, pp. 87-93, 2019. https://doi.org/10.1109/MWC.2019.1700441

[4] E. M. Idriss, A. Hakim, and A. Laghrib, “On the well-posedness of a tensor-based second order PDE with bilateral term for image super-resolution,” Evolution Equations and Control Theory, vol. 12, no. 2, pp. 703-731, 2023. https://doi.org/10.3934/eect.2022047

[5] H. Steele, A. Jack, and J. Liu, “Novel approach for validation of innovative modules for railway traffic management systems in a virtual environment,” Proceedings of the Institution of Mechanical Engineers, Part F: Journal of Rail and Rapid Transit, vol. 236, no. 2, pp. 139-148, 2022. https://doi.org/10.1177/095440972110418

[6] Q. Du, K. Huang, J. Scott, and W. Shen, “A space-time nonlocal traffic flow model: Relaxation representation and local limit,” Discrete and Continuous Dynamical Systems, vol. 43, no. 9, pp. 3456-3484, 2023. https://doi.org/10.3934/dcds.2023054

[7] C. Zhai, and W. Wu, “A macro traffic flow model with on-ramp considering driver's predictive effect,” Journal of Transportation Systems Engineering and Information Technology, vol. 20, no. 4, pp. 119-127, 2020. http://www.tseit.org.cn/EN/Y2020/V20/I4/119

[8] A. Hyochang, and C. Han-Jin, “Research of automatic recognition of car license plates based on deep learning for convergence traffic control system,” Personal and Ubiquitous Computing, vol. 27, no. 3, pp. 1139-1148, 2023. https://doi.org/10.1007/s00779-020-01514-z

[9] I. Finkelberg, T. Petrov, and A. Gal-Tzur, “The effects of vehicle-to-infrastructure communication reliability on performance of signalized intersection traffic control,” IEEE Transactions on Intelligent Transportation Systems, vol. 23, no. 9, pp. 15450-15461, 2022. https://doi.org/10.1109/TITS.2022.3140767

[10] N. Espitia, J. Auriol, H. Yu, and M. Krstic, “Traffic flow control on cascaded roads by event-triggered output feedback,” International Journal of Robust and Nonlinear Control, vol. 32, no. 10, pp. 5919-5949, 2022. https://doi.org/10.1002/rnc.6122

[11] Y. Zheng, J. Wang, and K. Li, “Smoothing traffic flow via control of autonomous vehicles,” IEEE Internet of Things Journal, vol. 7, no. 5, pp. 3882-3896, 2020. https://doi.org/10.1109/JIOT.2020.2966506

[12] Q. Liu, S. Wu, and P. Zhang, “Statistical analysis of urban traffic flow using deep learning,” Informatica, vol. 48, no. 5, pp. 23-28, 2024. https://doi.org/10.31449/inf.v48i5.5393

[13] J. Yu, “Passenger flow prediction of tourist attractions by integrating differential evolution and GWO,” Informatica, vol. 48, no. 13, pp. 31-50, 2024.

https://doi.org/10.31449/inf.v48i13.6159

[14] X. Ge, Q. L. Han, L. Ding, Y. L. Wang, and X. M. Zhang, "Dynamic event-triggered distributed coordination control and its applications: A survey of trends and techniques," IEEE Transactions on Systems, Man, and Cybernetics: Systems, vol. 50, no. 9, pp. 3112-3125, 2020. https://doi.org/10.1109/TSMC.2020.3010825

[15] S. Pu, W. Shi, J. Xu, and A. Nedić, "Push-pull gradient methods for distributed optimization in networks," IEEE Transactions on Automatic Control, vol. 66, no. 1, pp. 1-16, 2020. https://doi.org/10.1109/TAC.2020.2972824

[16] A. Laouzai, and R. Ouafi, "A prediction model for atmospheric pollution reduction from urban traffic," Environment and Planning B: Urban Analytics and City Science, vol. 49, no. 2, pp. 566-584, 2022. https://doi.org/10.1177/23998083211005776

[17] M. A. Envelope, G. F. Envelope, and R. M. Envelope, "Modelling and optimization of emissions in steady state urban traffic networks," IFAC-PapersOnLine, vol. 55, no. 5, pp. 31-36, 2022. https://doi.org/10.1016/j.ifacol.2022.07.635

[18] T. Okano, T. Nozaki, and T. Murakami, "An approach to evaluation index-based gain scheduling for acceleration-based four-channel bilateral control," Journal of the Japan Society for Precision Engineering, vol. 86, no. 9, pp. 720-730, 2020. https://doi.org/10.2493/jjspe.86.720

[19] Y. Jin, Z. Bi, and X. Qin, "Additive Gaussian noise model and Kalman filter to enhance controllability of gesture-controlled teleoperated soft actuators," Proceedings of the Institution of Mechanical Engineers, Part B: Journal of Engineering Manufacture, vol. 235, no. 14, pp. 2219-2229, 2021. https://doi.org/10.1177/0954405420941007

[20] E. S. Handayani, R. Susilowati, and I. Setyopranoto, "Transient bilateral common carotid artery occlusion (tBCCAO) of rats as a model of global cerebral ischemia," Bangladesh Journal of Medical Science, vol. 18, no. 3, pp. 491-500, 2019. https://doi.org/10.3329/bjms.v18i3.41616

[21] E. Estrada, W. Yu, and X. Li, "Stability and transparency of delayed bilateral teleoperation with haptic feedback," International Journal of Applied Mathematics and Computer Science, vol. 29, no. 4, pp. 681-692, 2019. https://doi.org/10.2478/amcs-2019-0050

[22] S. Pal, A. Roy, P. Shivakumara, and U. Pal, "Adapting a swin transformer for license plate number and text detection in drone images," Artificial Intelligence and Applications, vol. 1, no. 3, pp. 145-154, 2023. https://doi.org/10.47852/bonviewAIA3202549

Appendix

List of Abbreviations

Full name	Abbreviation
Traffic flow control	TFC
Intelligent traffic flow control	ITFC
Multi-Node Bilateral Control	MNBC
Predictable bilateral control model	PBCM
Convolutional neural networks	CNN
Process variables	PV
Set values	SV
Micro Doppler characteristics	MDC
Frequency Modulated Continuous Wave	FMCW
Generative Adversarial Network	GAN
Conditional Generative Adversarial Network	CGAN
Assisted Classification Generative Adversarial Network	ACGAN